CONF-830469--9

BNL-33221

QUASIELASTIC REACTIONS

BNL--33221

DE83 014616

OLE HANSEN
Brookhaven National Laboratory
Department of Physics
Upton, New York 11973

A brief review is presented of the experimental and theoretical situation regarding transfer reactions and inelastic scattering. In the first category there is little (very little) precision data for heavy projectiles and consequently almost no experience with quantitative theoretical analysis. For the inelastic scattering the rather extensive data strongly supports the coupled channels models with collective formfactors. At the most back angles, at intensities about 10^{-5} of Rutherford scattering, a second, compound-like mechanism becomes dominant. The description of the interplay of these two opposite mechanisms provides a new challenge for our understanding.

1. INTRODUCTION

If one observes a heavy ion scattering spectrum, say Fe+Sn, at an angle near grazing with a simple solid state detector, one will see two rather broad bumps. The most energetic bump is centered near a binary Q-value of zero and has an angular distribution that resembles elastic scattering. The bump typically covers the Q-value range from zero to minus 50 MeV. This part of the spectrum is referred to as the quasielastic part and is the subject of this talk. The second bump is the deep inelastic collisions. The above

description is valid for bombarding energies under, say, 15 or 20 MeV per nucleon.

2. TRANSFER REACTIONS

Let us look at the quasielastic spectrum with good mass and Z-resolution. We can then answer questions about the particle flow between projectile and target in a grazing collision. Figure 1 shows a comparison of data and theory from $^{56}Fe+^{64}Ni$ quasielastic reactions. First and second moments of A and N-Z are depicted against minus the binary Q-value. The data are represented by filled circles and the theory by open ones. The theory is the one-body dissipation model with Pauli-blocking by Randrup corrected for evaporation of the excited reaction fragments by Monte Carlo calculations. Data and theory are from ref. 1. The good agreement between experiment and theory mostly demonstrates that the evaporation corrections are reasonable, as one does not predict or observe any substantial mass flow in such a near symmetric system.

In the asymmetric $^{56}Fe+^{122}Sn$ case (Fig. 2), the observed (filled circles) $\langle N-Z\rangle$, $\sigma(A)$ and $\sigma(N-Z)$ agree quite well with theory (open circles), while for $\langle A\rangle$, theory underpredicts the average number of nucleons removed from the ^{56}Fe projectile. The discrepancy is with $\langle N\rangle$, which is predicted to be >30 and is observed to be smaller than 30. The full curves indicate the theoretical result before correction for evaporation. Thus, in the Sn case where some net flow is observed, the theory fails quantitatively.

If we attempt to look at a definite transfer reaction to a definite final state, there are simply no data at present for heavy systems ($A_1+A_2>80$). The closest we can

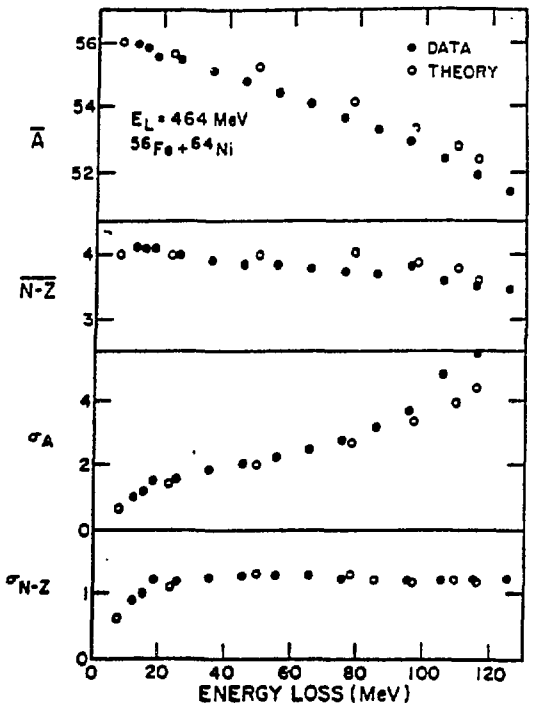

FIGURE 1 First and second moments of mass (A) and neutron excess (N-Z) for reaction products from $^{56}Fe+^{64}Ni$ plotted versus -Q-value (see ref. 1).

get is shown in Fig. 3, where the $^{208}Pb(^{86}Kr,^{87}Kr)^{207}Pb$ data[2] were observed with about 2 to 2.5 MeV energy resolution and thus covers a few ^{207}Pb and ^{87}Kr states. The DWBA curve from a neighboring reaction (between ground states) has been in the literature[3] since 1977 and indicates that the reaction kinematics of the DWBA is closely correct.

Another case, depicted in Fig. 4, shows one proton transfer data[1,4] to a 9 MeV broad energy range for the reaction $^{58}Ni(^{56}Fe,^{55}Mn)^{59}Cu$. The measured and DWBA calculated angular distributions agree well. Under the assump-

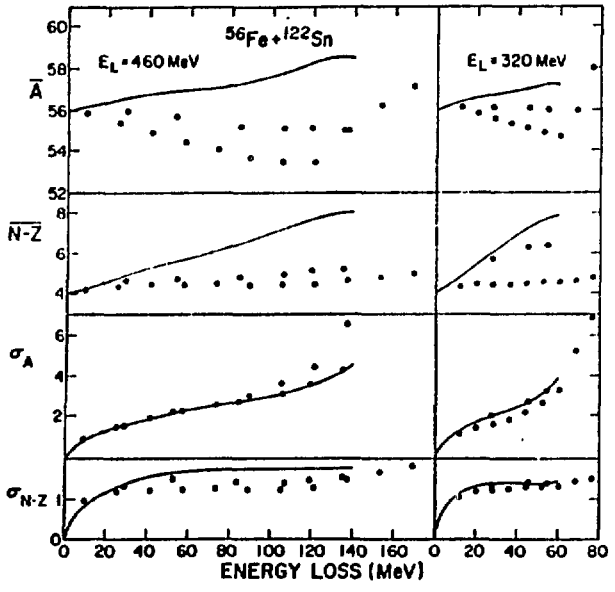

FIGURE 2 First and second moments of mass and neutron excess for reaction products from $^{56}Fe+^{122}Sn$ plotted versus -Q-value (see ref. 1).

tion that an $f_{7/2}$ proton is picked up from ^{56}Fe and transferred to the unoccupied orbits in the $28<Z\leq50$ major shell, the DWBA cross section summed over these orbits falls short of the observed cross section by a factor of two at 315 MeV and roughly by a factor of four at 460 MeV. Thus, given the somewhat undefined character of the data, the simple DWBA theory seems remarkably realistic.

Figure 5 shows the bulk systematics of transfer angular distributions, from left to right, one, two and three nucleon transfer. The Q-value decreases by 5 MeV for each distribution going from bottom toward top. The Gaussians fitted to the data show that the maximum cross section

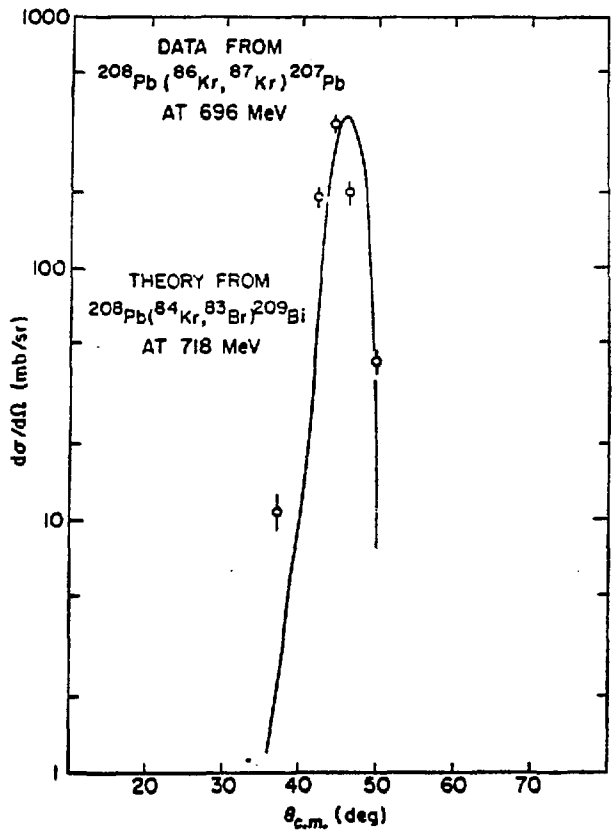

FIGURE 3 Angular distribution from the $^{208}Pb(^{86}Kr,^{87}Kr)^{207}Pb$ one neutron transfer reaction for ^{207}Pb excitations near zero.[2] The DWBA curve is for a "neighboring" reaction, taken from ref. 3.

moves forward with decreasing Q, and that the distributions get wider with decreasing Q and with increasing number of transferred particles; all pointing to a gradual shift from simple (one step) mechanisms to more complicated, multistep reactions. There are no quantitative theoretical predictions.

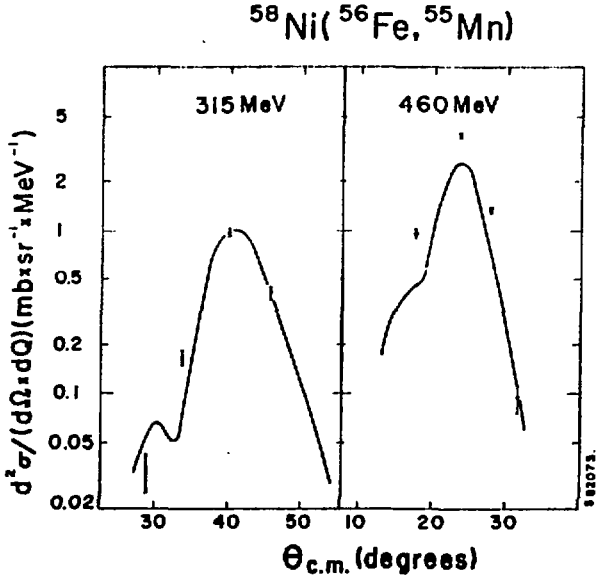

FIGURE 4 Angular distributions from the $^{58}Ni(^{56}Fe,^{55}Mn)$ ^{59}Cu reactions for $E_x<9$ MeV. The curves are DWBA calculations (see ref. 4).

This brief discussion shows that there exists a striking shortage of accurate, high resolution data, and of quantitative detailed theories. Figure 5 gives a gross view of the development of grazing reactions from simple stripping-like transfers to complicated transfers more reminiscent of deep inelastic collisions than of grazing encounters. A microscopic "energy loss" theory built on multiple step reactions seems overdue.

3. INELASTIC SCATTERING

The inelastic scattering process is much more selective than transfer processes and usually only two or three transitions

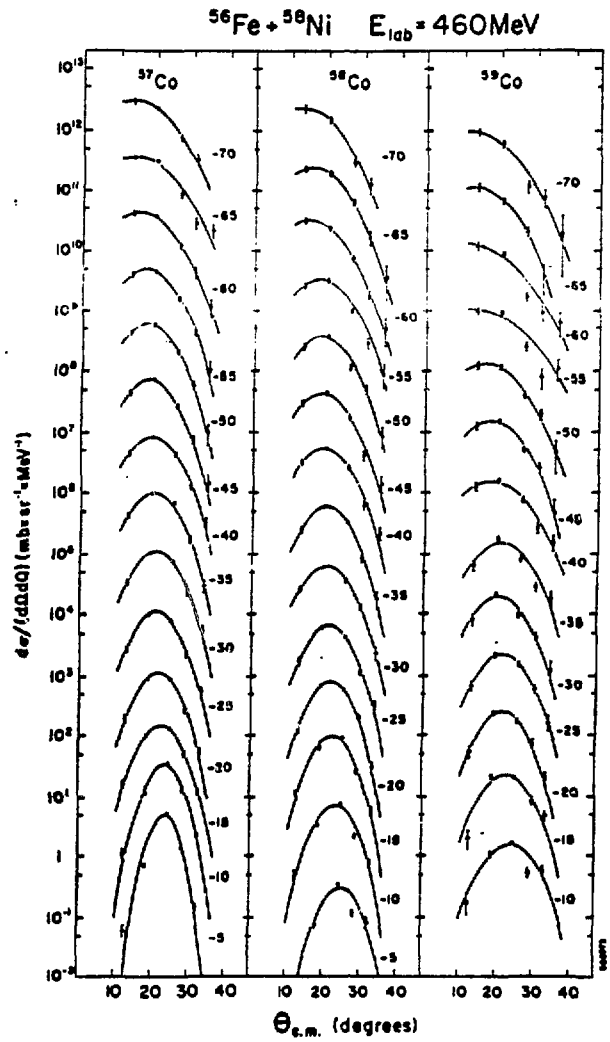

FIGURE 5 Systematics of angular distributions from 1, 2 and 3 nuclear transfer reactions induced by ^{56}Fe on ^{58}Ni. The Q value for the 5 MeV broad bin is given to the right of the Gaussian fit to the data. The cross section is obtained by multiplying the plotted one by $10^{Q/5}$ (see ref. 4).

are strong. Inelastic scattering experiments are therefore easier and high precision data much more abundant than for the transfer case. Also, the theoretical situation is better. The almost vanishing mass transfer makes recoil problems unimportant and the only important finite range effects are from Coulomb excitations and they can be handled accurately. Thus the direct reaction quantum mechanical coupled channels models provide an adequate framework that can be used for accurate numerical predictions (see, e.g. refs. 5,6).

Figure 6 shows results from a $^{60}Ni(^{28}Si,^{28}Si')$ experiment[7] at 5 A·MeV. The spectrum contains 5 inelastic lines, with the Si and Ni first 2^+ transitions as the dominant ones, followed by the mutual $2^+ + 2^+$ excitation. The ^{60}Ni 4^+ and 3^- transitions are not so collective[8] so the strongly coupled system consists of the ground states, and two 2^+ states. The fits to the angular distributions shown in Fig. 6 were obtained by using a standard Woods-Saxon potential (see ref. 7) and an interaction expanded to second order in the Si and Ni deformations. The nuclear deformation lengths for the two 2^+ states were adjusted to give a good fit to the elastic and 2^+ cross sections. The mutual excitation then contains no free parameters within the chosen reaction model, so the agreement with the data provide a strong confirmation of the model description.

The Si+Ni system is fairly strongly coupled; at the angle where $d\sigma(\text{elastic})/d\sigma(\text{Rutherford})$ is 1/4, the sum of the 2^+ transitions is ≈75% of the elastic cross section. The coupling has a marked effect on the elastic cross section. Figure 7 (taken from ref. 8) shows the elastic scattering angular distribution with a coupled channels fit (broken line) including the two single 2^+ excitations. The

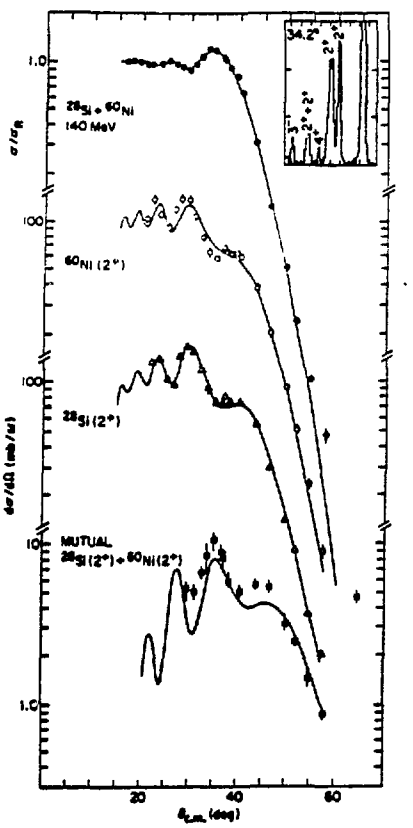

FIGURE 6 Angular distributions and coupled channels fits to $^{60}Ni(^{28}Si,^{28}Si')$ data (see ref. 7).

two other curves were obtained by switching off first the coupling to the Ni 2^+ state (fully drawn) and then also the Si coupling. At back angles the two latter calculations underpredict the measured cross section. Since the nuclear coupling is dominant at these angles, the figure demonstrates that the nuclear force provides a net de-excitation of the 2^+ states and returns flux to the elastic channel.

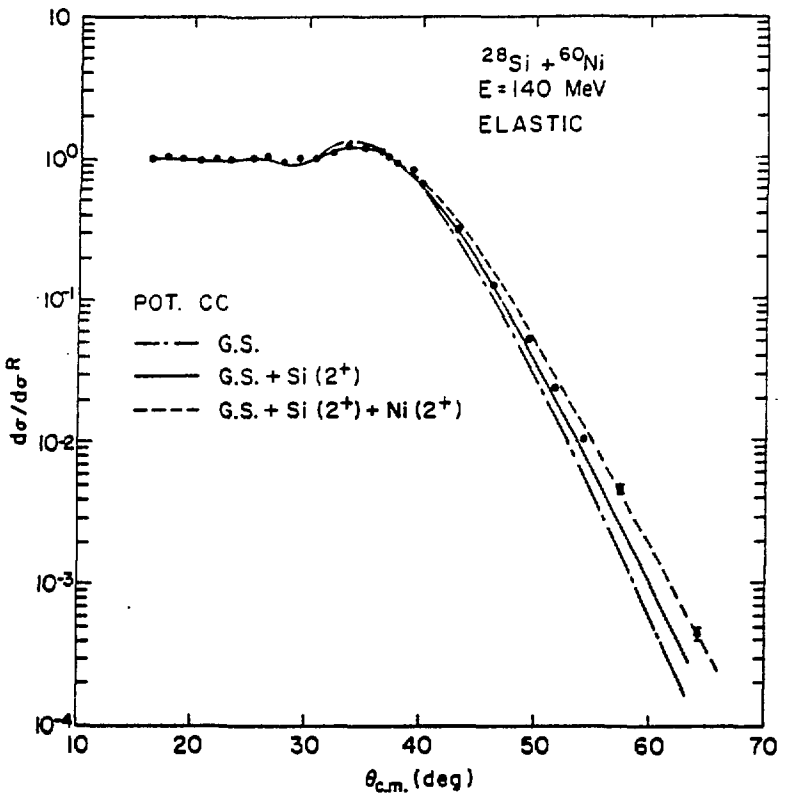

FIGURE 7 Elastic scattering from $^{60}Ni+^{28}Si$.

This result holds true quite generally, and is an example of the Coulomb-nuclear interference phenomenon (see also the discussions in refs. 9-11).

An example of a lighter, even more strongly coupled system is shown in Fig. 8, a spectrum from inelastic scattering of ^{28}Si from ^{28}Si. Here the inelastic 2^+ excitation is stronger than the elastic scattering and the mutual 2^+-2^+ channel is starting to compete with the elastic channel. The $^{28}Si+^{28}Si$ system has been studied at a number of energies, 80, 100, and 120 MeV at Argonne[13] and at 151.25 and 180 MeV at Brookhaven.[12] It is a general feature of the

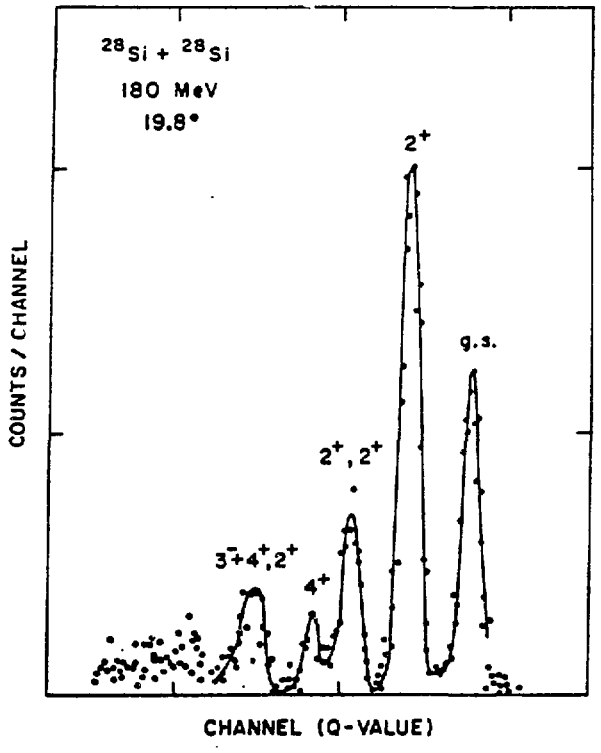

FIGURE 8 Spectrum from $^{28}Si(^{28}Si,^{28}Si')$ at 180 MeV and 19.8° lab angle. (Data from ref. 12).

spectra that at angles behind the quarter-point, the inelastic excitations start to dominate over elastic scattering and (see, e.f. ref. 14) at angles close to 90°, the mutual excitations become dominant.

Figures 9 and 10 show the elastic and inelastic 2^+ angular distributions at 151.25 MeV compared with coupled channels calculations,[12] the latter with a rotational model formfactor and including the $0^+ - 2^+ - 4^+$, and mutual $2^+ + 2^+$ couplings. The CC approach describes the data well over a cross section range of four orders of magnitude. Figure 11 shows the exponential fall-off of $^{28}Si+^{28}Si$ inelastic

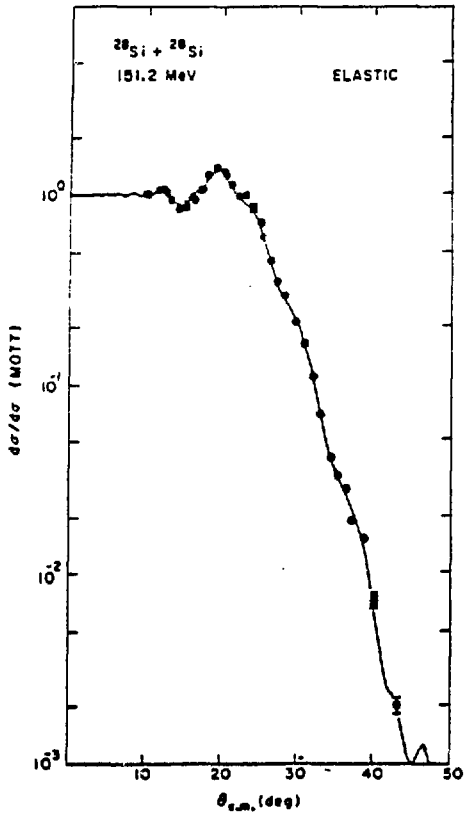

FIGURE 9 Elastic scattering angular distribution from $^{28}Si+^{28}Si$ at 151.2 MeV relative to Mott scattering. The curve through the points is a coupled channels fit to the data as explained in the text (from ref. 12).

angular distributions at angles backwards of the quarter-point. The elastic cross section falls off the fastest, followed by the 2^+ inelastic while the $2^+ + 2^+$ mutual excitation has the flattest slope. Thus as one goes to larger and larger angles, the inelastic spectrum will show an increasing dominance of the mutual excitation. The direct reaction model gives a simple explanation. The formfactors

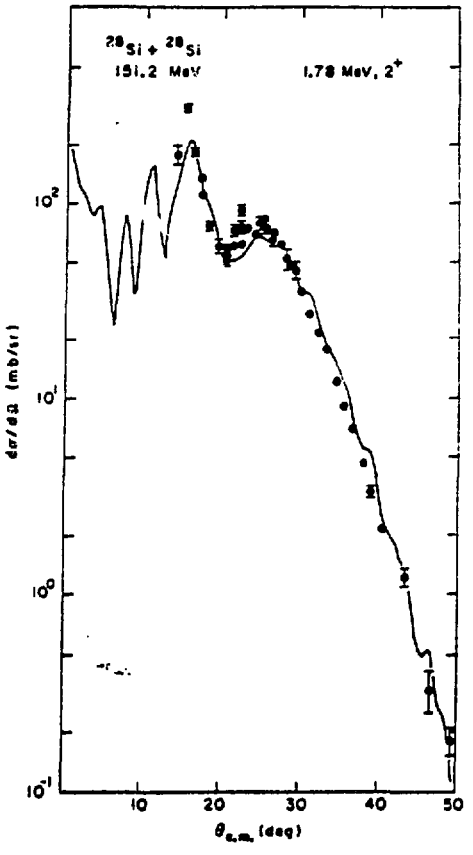

FIGURE 10 Inelastic scattering angular distribution from $^{28}Si+^{28}Si$ at 151.2 MeV corresponding to excitation of the 1.78 MeV 2^+ state.[12] The curve is a coupled channels fit to the data as explained in the text.

are essentially exponentials from the nuclear surface and further out. A second order process has a formfactor that is a product of two single step formfactors and thus the *second order formfactor is a steeper exponential than the* first order formfactor. As a consequence, fewer partial waves will contribute in second order processes than in first order ones, thus giving rise to flatter angular distributions for the second order process ($\Delta\theta x\Delta l$=constant).

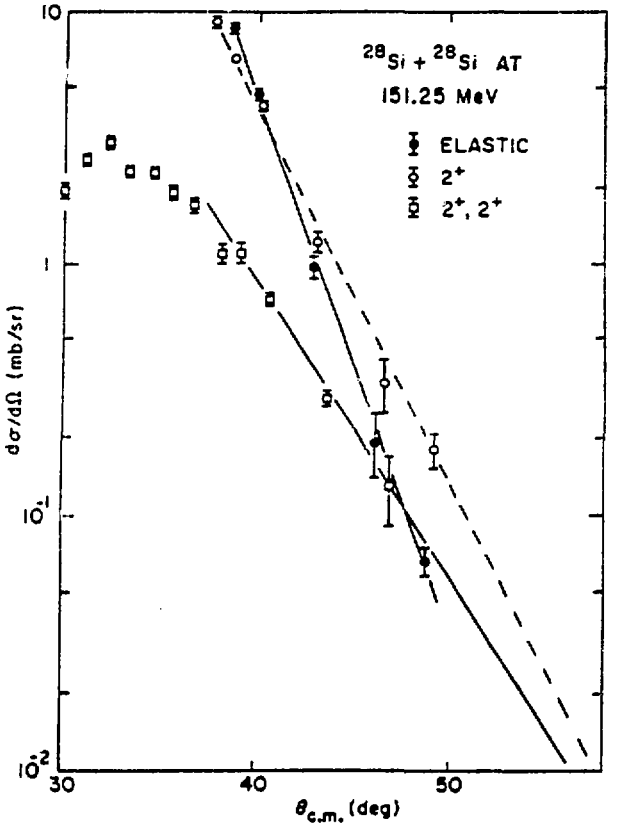

FIGURE 11 Angular distributions backwards of 30° c.m. from $^{28}Si+^{28}Si$ inelastic scattering at 151.25 MeV. The curves are drawn through the points to guide the eye. (Data from ref. 12).

[This argument is also valid for the transfer reactions discussed earlier.] One may thus see the change in the inelastic spectra with angle as a simple consequence of the direct character of the reaction process.

Figure 12, however, shows that this is not the full explanation. The elastic angular distribution[13] after 4 decades of exponential fall-off, breaks into strong oscil-

lations around a constant average. The inelastic angular distributions show a similar behavior. The coupled channels calculations decrease exponentially for almost two orders of magnitude below the value where the oscillations

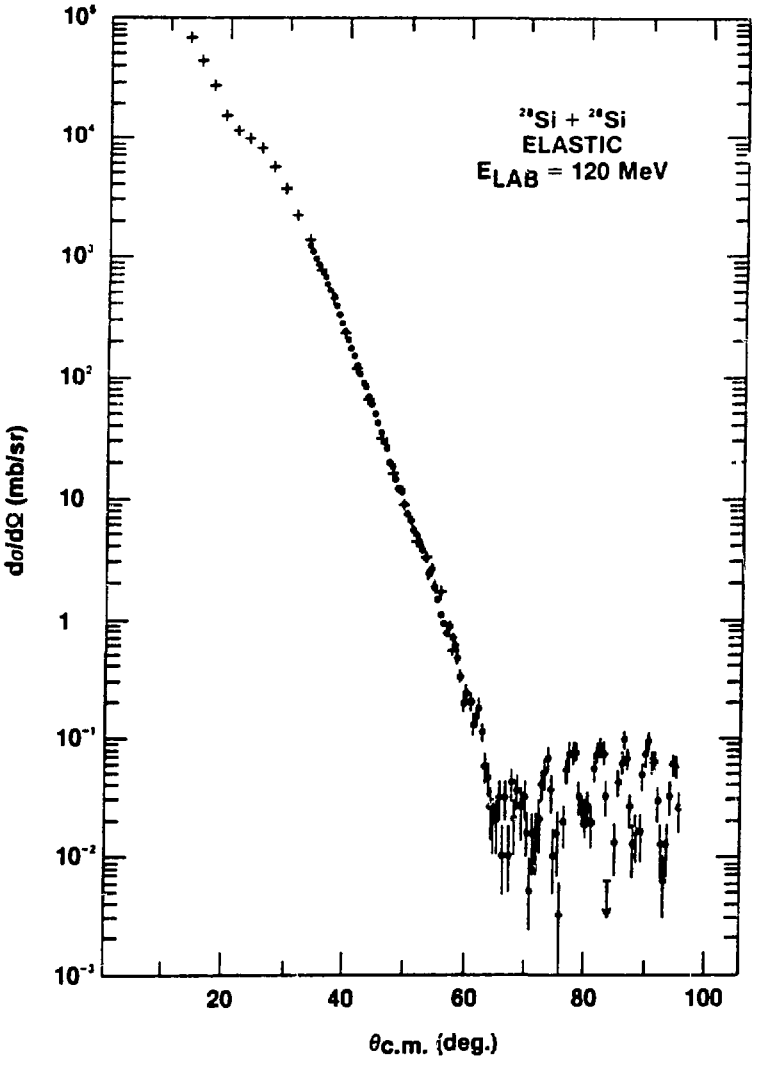

FIGURE 12 Angular distribution of $^{28}Si+^{28}Si$ elastic scattering at 120 MeV. (Data from ref. 13).

start, before the Mott scattering makes the angular distribution oscillate around a constant value. Change of the potential from strong absorption (needed to give the exponential fall-off) to a surface transparent potential can create oscillations at about the right cross section level and in the right angular range. However, the 4 decades of straight exponential decay are then lost. Also, the excitation functions in the 90^{o} region show narrow (<200 keV) resonances (see, R.R. Betts, invited talk) which cannot be reproduced by potential scattering.

Thus we are forced to accept that a different reaction mechanism dominates near 90^{o}, one that more fits the characteristics of a compound system. The smooth change in the spectrum with angle is paired with a dramatic change in the cross section angular distribution. The two types of reaction mechanism, multistep direct and compound-like, show the same selectivity in populating collective states and, in particular, mutual excitations.

There is presently not a single comprehensive model which explains this interplay between direct and compound in a quantitative way; but now there is at least data to demonstrate that the two opposite reaction mechanisms meet and interplay in a specific way. At 120 MeV the centroid of the inelastic spectra[14] is close to where the mutual 4+6 and 6+6 excitation should occur (although these cannot be uniquely identified in the data), and those spins are close to what one expects from a rotating dinucleus, i.e. 1/7 of the total spin which is near 40$\hbar$. A provocative result, that leads one to think of a connection with fission and deep inelastic collisions.

ACKNOWLEDGEMENTS

I am indebted to F. Videbaek for the coupled channels analyses for $^{28}Si+^{28}Si$ inelastic scattering, and to P.D. Bond for the ^{86}Kr transfer data. The talk has benefited enormously from discussions with A.J. Baltz, R.R. Betts, P.D. Bond, F. Videbaek, and Aa. Winther. This work was supported by the U.S. Department of Energy under Contract No. DE-AC02-76CH00016 with the Brookhaven National Laboratory.

REFERENCES

1. H.C. BRITT et al., Phys. Rev. C26, 1999 (1982).
2. P.D. BOND et al., to be published.
3. A.J. BALTZ, Phys. Rev. Lett. 38, 1197 (1977).
4. S. PONTOPPIDAN et al., Phys. Rev. C (to be published).
5. A.J. BALTZ, Phys. Rev. C25, 240 (1982).
6. M. RHOADES-BROWN et al., Phys. Rev. C21, 2417 (1980).
7. P.R. CHRISTENSEN et al., Phys. Lett. 114B, 423 (1982).
8. P.R. CHRISTENSEN et al., Phys. Rev. C (in print).
9. K.E. REHM et al., Phys. Rev. Lett. 40, 1479 (1978).
10. R.S. ASCUITTO et al., Phys. Rev. Lett. 41, 1159 (1978).
11. A.J. BALTZ and P.D. BOND, Phys. Lett. (in print).
12. F. VIDEBAEK et al., (to be published).
13. R.R. BETTS et al., (to be published).
14. R.R. BETTS et al., Phys. Rev. Lett. 46, 313 (1981).